

# *In Vivo* Evaluation of a Nanoantibiotic-Integrated Collagen-Chitosan Scaffold for Bone Regeneration in a Critical-Size Rat Defect Model

**Nora Azirah Mohd Zayi<sup>1</sup>, Muhammad Lutfi Mohamed Halim<sup>1</sup>, Ahmad Fahmi Harun Ismail<sup>1,5</sup>, Mohd Hafiz Arzmi<sup>2,3,5</sup>, Pram Kumar A/L Subramaniam<sup>4</sup>, Mohd Yusof Mohamad<sup>1,5,\*</sup>**

<sup>1</sup>Department of Physical Rehabilitation Sciences, Kuliyah of Allied Health Sciences, International Islamic University Malaysia, Pahang, Malaysia

<sup>2</sup>Department of Fundamental Dental and Medical Science, Kuliyah of Dentistry, International Islamic University Malaysia, Pahang, Malaysia

<sup>3</sup>Melbourne Dental School, The University of Melbourne, Victoria, Australia

<sup>4</sup>Department of Oral Maxillofacial Surgery and Oral Diagnosis, Kuliyah of Dentistry, International Islamic University Malaysia, Pahang, Malaysia.

<sup>5</sup>Cluster of Cancer Research Initiative IIUM (COCRII), International Islamic University Malaysia, Pahang, Malaysia

## ABSTRACT

**Background:** Bone loss due to periodontal disease, trauma, or anatomical factors is a significant challenge in periodontology. Guided Bone Regeneration (GBR) scaffolds, which provide a 3D structure for cell attachment and tissue regeneration, have shown promise in treating bone defects. However, non-biodegradable scaffolds require secondary surgery for removal, which can increase the risk of infection and hinder bone regeneration. Biodegradable scaffolds with antibacterial properties offer a solution to reduce infection risk and promote healing. The use of antibiotic-loaded scaffolds, such as metronidazole nanoparticle-loaded (MNP) scaffolds, can address the issue of prolonged antibiotic use and associated risks like resistance and side effects. Previous studies have demonstrated the potential of MNP-loaded scaffolds in periodontal regeneration. This study aims to evaluate the effectiveness of a collagen-chitosan scaffold loaded with metronidazole nanoparticles, focusing on its *in vivo* biocompatibility and potential toxicity. **Materials and Methods:** A sample of 18 rats was chosen based on the Resource Equation Method, ensuring an adequate sample with a 20% attrition rate, in line with animal testing ethics (3Rs: replacement, reduction, refinement). Male Sprague-Dawley rats (8 weeks, 250-300g) were divided into three groups: CC-MNP scaffold, CC scaffold, and no scaffold (control). Anaesthesia was given intraperitoneally using ketamine (80 mg/kg) and xylazine (10 mg/kg). A 5 mm skull defect was created surgically, and the respective scaffold treatment was placed. The surgical site was closed, and post-operative monitoring focused on pain and healing for four weeks, after which X-ray imaging assessed bone healing at the defect site. Radiographic images were analyzed using Image J, measuring new bone formation percentage as a function of the original defect size. Bone regeneration was quantified by defect closure area based on ROI measurements. Histological analysis on decalcified tissue sections stained with hematoxylin and eosin (H&E) was conducted to evaluate new bone morphology. **Results:** The CC-MNP scaffold group demonstrated significantly higher rates of bone organisation compared to the CC scaffold and control groups. Histological analysis showed denser and more compact bone regeneration within the defect area, suggesting that the MNP-infused scaffold promotes cellular activity and tissue integration. This study underscores the potential of a biodegradable, antibiotic-loaded scaffold to support bone regeneration in critical defects, reducing the need for secondary surgeries and offering a sustainable solution potentially suitable for clinical use in periodontal applications.

## Keywords:

Bone regeneration; Periodontal disease, Biodegradable scaffold; collagen-chitosan scaffold; metronidazole nonantibiotics

## INTRODUCTION

Bone loss resulting from periodontal disease, trauma, or anatomical factors poses a common therapeutic challenge in the field of periodontology (Donos et al., 2015). To promote bone regeneration in various types of bone defects under different systemic conditions, a range of bone grafts, bone substitutes, biomaterials, or combined regenerative procedures have been employed. Guided Bone Regeneration (GBR) scaffolds, which provide a three-dimensional (3D) structure for cell attachment, growth, and tissue regeneration, have been widely studied for the treatment of periodontal disease (Lim et al., 2019).

One of the common challenges with GBR application is the use of non-biodegradable scaffolds, which do not degrade naturally within the body over time. As a result, a second surgical procedure is often required to remove the scaffold once bone regeneration is complete. After scaffold removal, the site becomes exposed, creating a favourable environment for bacterial colonisation and an increased risk of infection. This bacterial colonisation can hinder the natural bone regeneration process by causing inflammation and tissue damage. To address these limitations, biodegradable scaffolds with antibacterial properties have been developed.

These scaffolds aim to reduce the risk of infection, promote a more conducive environment for bone regeneration, and ultimately improve the outcomes of GBR treatments. Biodegradable scaffolds are commercially available; however, the halal status of these commercially available scaffolds remains uncertain, particularly regarding the materials and their source. As tissue engineering for bone regeneration continues to grow, it is crucial that scaffolds meet halal standards for Muslim populations while also reducing the risk of infection.

Prolonged use of antibiotics can increase the risk of systemic side effects, including antibiotic resistance, potentially compromising the success of GBR procedures. A promising approach to overcome this issue is the development of scaffolds loaded with antibiotic nanoparticles, such as metronidazole nanoparticle-loaded (MNP) scaffolds. Previous studies have demonstrated the potential of MNP loaded scaffolds, particularly their ability to provide controlled and sustained drug release at the site of infection, minimising the risks associated with systemic antibiotic use, such as resistance and side effect. For instance, a study by Zayi et al. (2023) developed a fish-derived collagen scaffold incorporated with metronidazole nanoparticles, demonstrating favorable physical characteristics, biodegradability, and swelling ability, which shown potential for their application in periodontal bone regeneration. In this study, we further evaluate the suitability and effectiveness of a collagen-chitosan scaffold loaded with metronidazole nanoparticles for periodontal regeneration, focusing specifically on the biomaterial's *in vivo* biocompatibility and potential toxicity.

## MATERIALS AND METHODS

### Development of Collagen-Chitosan Scaffold loaded with Metronidazole

The fabrication of collagen-chitosan scaffolds loaded with metronidazole nanoparticles (CC-MNP) followed the protocol outlined in a previous study. Certified halal fish collagen derived from *Tilapia mossambica* (Eva Chemicals, Kuala Lumpur, Malaysia) was utilised. A 30:70 collagen-to-chitosan ratio was prepared by dissolving the materials in a 1% glacial acetic acid solution (w/v). Glycerin (20%) was added as a plasticiser and stirred at room temperature for one hour. Neutralisation was achieved using 5% sodium bicarbonate (NaHCO<sub>3</sub>), and MNP at concentrations (30 wt%) were incorporated into the mixture. The blend was transferred to 96-well moulds, subjected to slow freezing at temperatures between -20°C and -80°C overnight, and subsequently freeze-dried for 24 hours. The lyophilised scaffolds were crosslinked through dehydrothermal treatment (DHT) at 105°C for 24 hours.

## Experimental Design and Procedure

The Sprague-Dawley rat skull defect model was used in this study, with sample size calculated based on the Resource Equation Method by Charan & Kantharia (2013). A total of 18 animals, male Sprague-Dawley rats, approximately eight weeks old and weighing between 250 and 300 grams, were divided into three groups for examination on the 4th weeks post-surgery, as shown in **Table 1**. In total, 18 animals were allocated across three groups, inclusive of a 20% attrition rate.

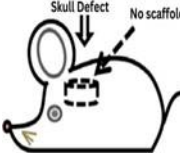
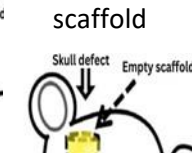
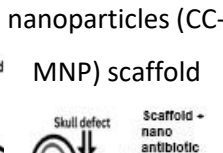
The study design involved three groups, each to be evaluated at 4 weeks post-surgery:

Group A: Rats with skull defects left untreated, serving as the control group to evaluate the natural healing process without any scaffold.

Group B: Rats with skull defects implanted with a collagen-chitosan (CC) scaffold. This group was used to assess the potential of a biodegradable scaffold for promoting bone regeneration without the addition of metronidazole nanoparticles.

Group C: Rats with skull defects implanted with a collagen-chitosan scaffold loaded with metronidazole nanoparticles (CC-MNP). This group was included to evaluate the combined effects of the scaffold and the localized antibiotic delivery system for enhanced bone regeneration and infection prevention.

**Table 1:** Study design

Groups	A	B	C
	Rats' skull defect without any scaffold implantation	Rats' skull defect implanted with collagen-chitosan (CC) scaffold	Rats' skull defect implanted with collagen-chitosan loaded with metronidazole nanoparticles (CC-MNP) scaffold
(n = 6)			

## Anaesthesia and Surgical Procedure

Anesthesia was administered using ketamine (80 mg/kg) and xylazine (10 mg/kg) to ensure deep sedation without pain responses. After shaving and disinfecting the animals' skulls with 10% polyvinylpyrrolidone (PVP), a 4 cm incision was made along the midline of the scalp to expose the skull. A 5 mm diameter defect was drilled into the skull using a trephine bur. A hydrated scaffold was then placed over the defect, and the surgical site was sutured with absorbable sutures according to the protocol by Carlos et al. (2020). Each animal was housed individually with free access to food and water. The procedure is approved by the IIUM Institutional Animal Care and Use Committee (I-ACUC) (IACUC 2023-013).

## Post-operative Observation

Rats were observed every 12 hours for the first 48 hours post-surgery and every other day afterwards. The pain was assessed based on guidelines from the University of Michigan's Unit for Laboratory Animal Medicine and the IACUC-IIUM Code of Practice, paying special attention to signs like arching, twitching, and aggression. The surgical wound was examined for signs of infection, including haemorrhage, scabbing, discharge, and swelling (Grant, 2009; Lansdown & Rowe, 2001).

## Animal Sacrifice

Euthanasia was performed using CO<sub>2</sub> gas in a chamber pre-filled to a 20-30% concentration, gradually increased to 70-100% to ensure humane termination (Moody et al., 2014). Mortality was confirmed by the absence of vital signs, after which skull samples were fixed in 10% formalin for further examination.

## In vivo X-ray

At the end of the 4th week, rats were euthanised and underwent X-ray imaging to assess scaffold efficacy in promoting defect healing. Imaging parameters were set for small animals (mFX-1000, FUJIFILM, Tokyo, Japan) with images focusing on the defect site. Bone regeneration was measured using Image J software, calculating new bone formation as a percentage of the initial defect area:

$$\% \text{ Bone Regeneration} = \frac{(\text{Initial ROI area} - \text{Final ROI area})}{(\text{Initial ROI area})} \times 100 \quad (1)$$

## Histological Analysis

Following X-ray analysis, tissue samples were processed for histological evaluation. The skull defects were decalcified in 17% EDTA, dehydrated, and embedded in paraffin. Sections approximately 5µm thick were stained with hematoxylin and eosin (H&E) and examined microscopically (Carlos et al., 2020; Ma et al., 2016).

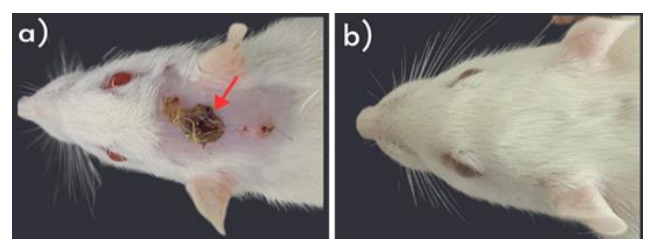
## RESULTS AND DISCUSSION

The critical size defect (CSD) is a fundamental concept when creating bone defect models, as it represents a bone defect that cannot heal spontaneously and instead forms fibrous connective tissue. CSDs require the application of a bone graft or substitute material to facilitate healing (Mukherjee et al., 2022; Zain & Hamdan, 2021). The term was first defined by Schmitz and Hollinger (1986) as "the smallest size intraosseous wound in a particular bone and animal species that will not naturally heal during the lifetime of the animal." In rat calvarial defects, a CSD of 5-8 mm is frequently used, allowing for successful regeneration within four weeks with intervention (Schmitz et al., 2018; Spicer et al., 2012; Ma et al., 2016).

This study utilized a 5 mm CSD in the rat calvarium, with no bone regeneration observed within the defect area in the absence of intervention, as shown in Figures 3a and 4a. This observation establishes a clear baseline for evaluating the effectiveness of the biomaterials used in this study.

## Post-operative observation & Wound Healing

No behavioural differences were observed between the control and experimental groups, showing effective post-operative care. By week 2, healing varied: the control group displayed redness and swelling, while scaffold-treated groups showed wound closure without inflammation. The accelerated healing in scaffold-treated groups is credited to metronidazole nanoparticles, which acted as antimicrobials, reducing infection and promoting recovery (El-Shanshory et al., 2022). By week 4, the redness had diminished across all groups, and fur regrowth indicated successful skin and epidermal layer healing, signalling to restore normal skin function as depicted in **Figure 1**. Scab formation is crucial in wound healing, controlled bleeding, blocking contamination, and protecting underlying tissues. In the final proliferative phase (lasting from days 4 to 14), new granulation tissue and extracellular matrix formed, supporting skin regeneration (Desmiaty et al., 2024).



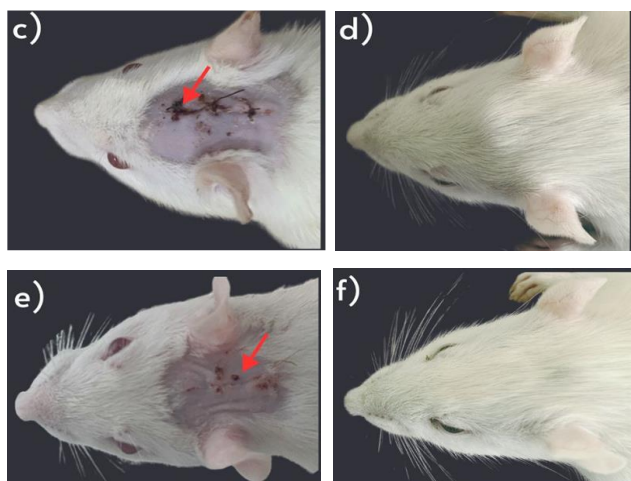


**Figure 1:** Photographs showing the wound area in all groups; non-implanted (a-b), implanted with CC-scaffold (c-d), and implanted with CC-MNP scaffold (e-f) at the week 2 and week 4.

**Table 2:** Analysis of Skin Abnormalities

Groups	Week 2	Week 4
Non-implanted	Large scab covering wound (red arrow) Visible inflammation and tissue damage Slow/incomplete healing	- Wound mostly healed - No scab visible - Fur regrowth observed in the wound area
Implanted with CC scaffold	- Partial wound closure - Smaller scab than non-implanted - No inflammation	- Complete wound closure - Minimal signs of wound - Fur regrowth observed
Implanted with CC-MNP scaffold	- Wound nearly healed - No scab and inflammation - Accelerated healing compared to other groups	Complete wound closure No scab or inflammation - Fur regrowth observed, suggesting full recovery

Table 2 presents the analysis of skin abnormalities at weeks 2 and 4. At week 2, the non-implanted group displayed a large scab covering the wound with visible inflammation and slow, incomplete healing. In contrast, rats implanted with the CC scaffold showed partial wound closure and smaller scabs with no inflammation. The CC-

MNP scaffold group exhibited the most advanced healing, with nearly healed wounds and no scab or inflammation. By week 4, the control group showed minimal scab presence, with fur regrowth indicating that the wound was mostly healed. The CC scaffold group achieved complete wound closure, with minimal signs of a wound, and fur regrowth observed. The CC-MNP scaffold group demonstrated complete wound closure, no scab or inflammation, and fur regrowth, suggesting full recovery.

Fur regrowth across all groups indicated significant healing, with the CC-MNP scaffold group demonstrating the fastest recovery, especially at week 2. This improvement is attributed to the metronidazole nanoparticles, which functioned as antimicrobials, inhibiting microbial growth and promoting an environment conducive to tissue regeneration. These findings are consistent with previous studies where metronidazole-loaded nanofibrous scaffolds enhanced wound healing by reducing microbial activity and supporting granulation tissue formation (El-Shanshory et al., 2022), as depicted in Figure 1e. In contrast, the non-implanted control group exhibited thicker scabs and residual debris, characteristic of early-phase wound healing (Choudhary et al., 2024), as shown in Figure 1a.

### Radiological Observation

The study assessed the percentage of bone regeneration under various conditions, as illustrated in **Figure 2**. The control group without scaffold implantation exhibited minimal bone regeneration ( $16.79\% \pm 2.99$ ), consistent with previous research, which suggests that natural healing is limited without biomaterial support (Togari et al., 2012). The defect in the control group remained largely unhealed, highlighting the body's limitations in repairing large bone defects without structural support. By contrast, groups receiving scaffold implants showed significantly improved outcomes, underscoring the necessity of a structural matrix for effective tissue regeneration (Daeifarshbaf et al., 2014; Hatakeyama et al., 2013; Kashe et al., 2021). The CC scaffold group achieved nearly complete regeneration ( $97.45\% \pm 0.51$ ), indicating that even a simple scaffold framework can support the natural healing process by providing a structure for cellular infiltration and tissue development. Prior studies support that biodegradable scaffolds facilitate bone growth and defect closure (Suvarnapathaki et al., 2022). Additionally, the CC-MNP scaffold group demonstrated nearly full bone regeneration ( $99.08\% \pm 0.76$ ), highlighting the role of bioactive nanoparticles in enhancing healing. **Figure 3** presents X-ray images of the bone defects. The control group's defect area remained largely unhealed, while the CC scaffold and CC-MNP scaffold groups showed



progressive bone formation, filling the entire defect area in the CC-MNP group. **Figure 4** shows ROI (Region of Interest) images, visually confirming these differences, with the CC-MNP scaffold group demonstrating near-total defect closure. The enhanced osteogenesis observed in the CC-MNP scaffolds likely due to the nanoparticles influencing cellular behaviours such as proliferation and differentiation, thus providing both mechanical support and the potential for therapeutic agent delivery.

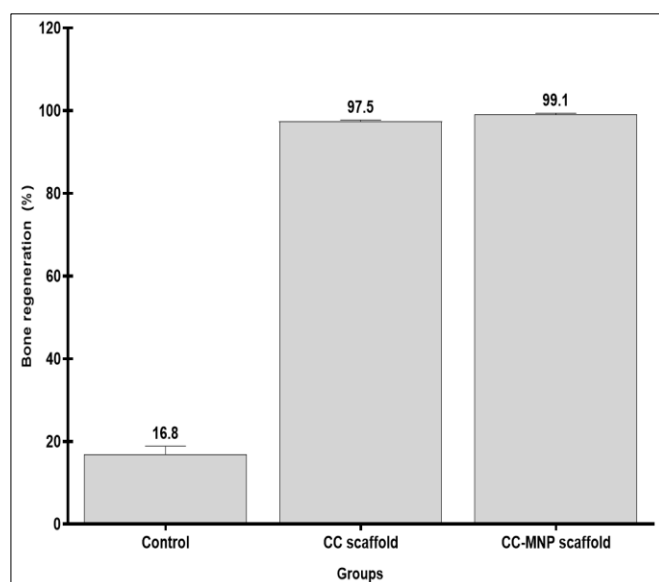


**Figure 2:** Percentage of bone regeneration in the rat skull defect area for the control group (no scaffold implantation) and groups implanted with scaffolds, without and with metronidazole (CC empty and CC-MNP scaffolds).

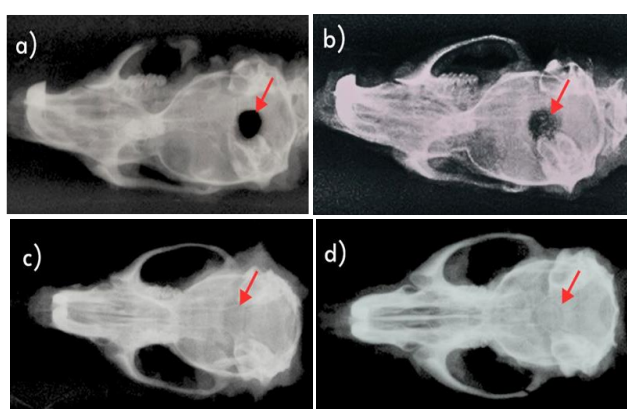


**Figure 3:** Error signs highlight the X-ray images of the defect area. (a) Baseline of the bone defect prior to treatment, (b) X-ray of the bone defect in a rat without any implantation, (c) newly formed bone at the defect closure in rats implanted with CC scaffold, and (d) newly formed bone at the defect closure in rats implanted with the CC-MNP scaffold

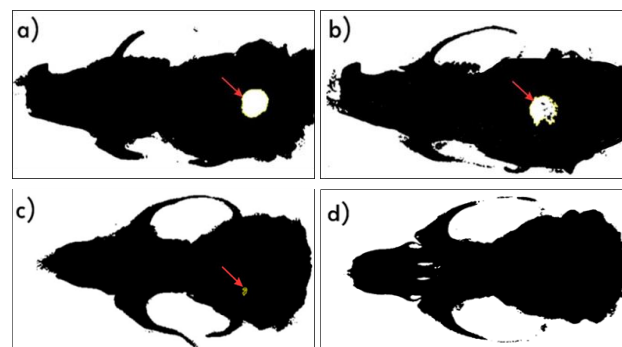


**Figure 4:** Error signs highlight the ROI images of the defect area using ImageJ. (a) Baseline of the bone defect, (b) the rat without any implantation, (c) newly formed bone at defect closure in rats implanted with an CC scaffold and (d) CC-MNP scaffold

### Histological analysis

The histological analysis in **Figures 5** and **6** illustrates bone regeneration across experimental groups. Rats with CC-MNP scaffolds, CC scaffolds, and without any scaffold were examined using haematoxylin and eosin (H&E) staining. Comparing baseline, control, CC scaffold, and CC-MNP scaffold groups highlighted the scaffolds' role in enhancing bone healing. In the baseline (**Figure 5a**), no new bone formed, and the defect remained largely unfilled, marked only by old bone (OB) on each side. By the 4th week, the control group (**Figure 5b**) showed fibrous tissue (FT) but no new bone (NB), consistent with X-ray findings and prior studies (Ono et al., 2014; Sun et al., 2018). This result aligns with earlier findings where natural healing without scaffolds was limited to soft tissue infiltration rather than bone regeneration (Chen et al., 2013), indicating that critical-size defects require scaffolds or bioactive agents for effective healing (Zhou & Lee, 2016).

In contrast, both scaffold-treated groups demonstrated notable bone formation. The CC scaffold provided a framework for new bone growth, facilitating the natural healing process by offering structural support and cellular infiltration space, as shown in previous studies (Sato et al., 2020). By week four, the CC-MNP scaffold group exhibited a more organised, dense new bone structure (**Figure 5d**), compared to the less organised bone in the Cc scaffold group (**Figure 5c**). Histological images showed NB formation, with a well-organised matrix and increased cell density. OB integrated seamlessly with NB, indicating active remodelling, similar to prior studies (Farazin & Mahjoubi, 2024).

Histological images at four weeks post-implantation

(Figure 6) further confirm these findings, revealing evidence of active remodelling. This is consistent with studies involving poly (L-lactic acid)-hydroxyapatite-gelatin scaffolds that similarly promoted osteogenesis and remodelling through osteoblast proliferation and osteoid matrix formation (Kashte et al., 2021). Previous studies have shown bacterial infections can hinder bone repair due to inflammation, often requiring prolonged antibiotic treatment or multiple surgeries. The nano-antibiotics in the scaffold may have reduced bacterial colonisation at the defect site, creating a favourable environment for bone healing (Farazin & Mahjoubi, 2024). The bioactive nanoparticles in the scaffold promoted mineralised matrix formation, accelerating regeneration and producing superior bone formation (Dasari et al., 2022).

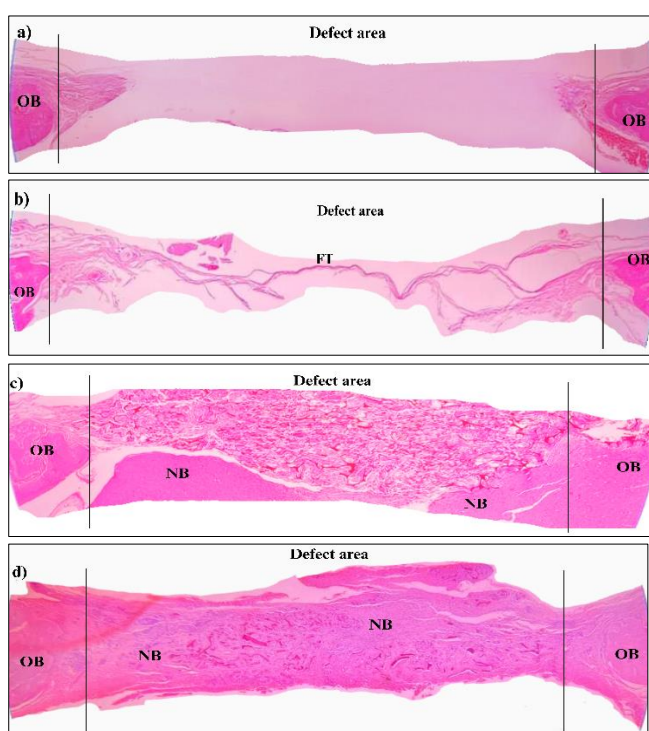


**Figure 5:** Histological images showing bone regeneration in rat skull defect areas under different conditions (a) shows the control group at baseline (0 weeks), with the presence of old bone (OB) and fibrous tissue (FT). (b) shows the same control group at 4 weeks, highlighting OB and FT. (c) displays rats implanted with a CC scaffold at 4 weeks, showing the presence of old bone (OB) and new bone (NB) in the defect area. (d) shows rats implanted with a CC-MNP scaffold at 4 weeks, demonstrating extensive new bone (NB) formation alongside old bone (OB) in the defect area (4x magnification).

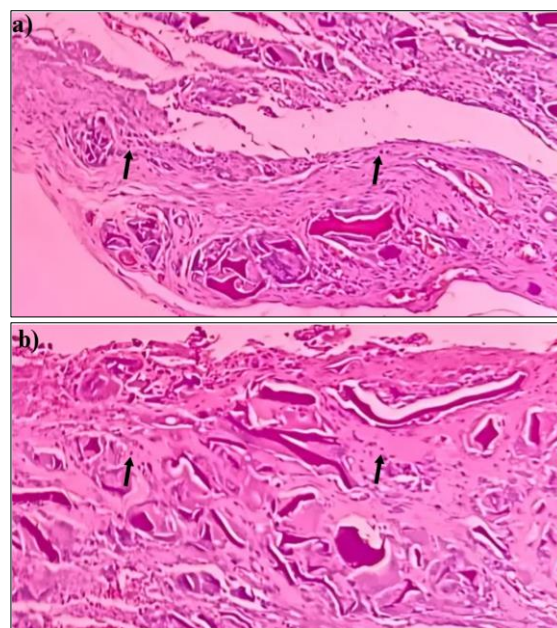


**Figure 6:** Histological images of rat bone sections at 4 weeks post-implantation. (a) CC scaffold group; (b) CC-MNP scaffold group. Arrows indicate osteocytes within the bone matrix at 100x magnification.

## CONCLUSION

The study highlighted significant bone healing improvements when using CC-MNP scaffolds compared to CC scaffolds. Although X-rays showed no major difference in bone healing between scaffold types, detailed analysis indicated denser and more organised bone growth in MNP-loaded scaffolds, suggesting that MNP supports enhanced cellular activity and bone quality. Minimal bone growth in the non-scaffold group underscores the importance of scaffolds in repairing larger bone defects. These findings suggest that the incorporation of MNP into scaffolds can improve structural integrity and cellular response, making MNP-loaded scaffolds a promising option for bone tissue repair.

## ACKNOWLEDGEMENT

This research was funded by the Ministry of Higher Education, Malaysia through the Fundamental Research Grant Scheme (FRGS) for Project ID: FRGS/1/2019/SKK14/UIAM/03/3

## REFERENCES

Carlos, C. R., Astarita, C., D'Aquino, R., & Pelegrine, A. A. (2020). Evaluation of bone regeneration in rat calvaria using bone autologous micrografts and xenografts: Histological and histomorphometric

- analysis. *Materials*, 13(19), 1–15. <https://doi.org/10.3390/MA13194284>
- Chalikias, S., Papaioannou, N., Koundis, G., Pappa, E., Galanos, A., Anastassopoulos, G., Sarris, I. N., Panteliou, S., Chronopoulos, E., & Dontas, I. A. (2021). Evaluation of femoral bone fracture healing in rats by the modal damping factor and its correlation with peripheral quantitative computed tomography. *Cureus*, 13(2). <https://doi.org/10.7759/cureus.13342>
- Chang, Y.-T., Lai, C.-C., & Lin, D.-J. (2023). Collagen scaffolds laden with human periodontal ligament fibroblasts promote periodontal regeneration in SD rat model. *Polymers*, 15(12), 2649. <https://doi.org/10.3390/polym15122649>
- Charan, J., & Kantharia, N. (2013). How to calculate sample size in animal studies? *Journal of Pharmacology and Pharmacotherapeutics*, 4(4), 303–306. <https://doi.org/10.4103/0976-500X.119726>
- Chhabra, S., Chhabra, N., Kaur, A., & Gupta, N. (2017). Wound healing concepts in clinical practice of OMFS. *Journal of Maxillofacial and Oral Surgery*, 16(4), 403–423. <https://doi.org/10.1007/s12663-016-0880-z>
- Chen, M. X., Zhong, Y. J., Dong, Q. Q., Wong, H. M., & Wen, Y. F. (2021). Global, regional, and national burden of severe periodontitis, 1990–2019: An analysis of the Global Burden of Disease Study 2019. *Journal of Clinical Periodontology*, 48(9), 1165–1188. <https://doi.org/10.1111/jcpe.13506>
- Choudhary, V., Choudhary, M., & Bollag, W. B. (2024). Exploring skin wound healing models and the impact of natural lipids on the healing process. *International Journal of Molecular Sciences*, 25(7). <https://doi.org/10.3390/ijms25073790>
- Cross, H. (2003). *Wound Care For People Affected by Leprosy: A Guide for Low Resource Situations*. 143. [http://www.ilep.org.uk/fileadmin/uploads/Documents/Infolep\\_Documents/Self\\_care/Wound\\_Care.pdf](http://www.ilep.org.uk/fileadmin/uploads/Documents/Infolep_Documents/Self_care/Wound_Care.pdf)
- Dasari, A., Xue, J., & Deb, S. (2022). Magnetic nanoparticles in bone tissue engineering. *Nanomaterials*, 12(5), 757. <https://doi.org/10.3390/nano12050757>
- Daei-farshbaf, N., Ardeshirylajimi, A., Seyedjafari, E., Piryaei, A., Fadaei Fathabady, F., Hedayati, M., Salehi, M., Soleimani, M., Nazarian, H., Moradi, S. L., & Norouzian, M. (2014). Bioceramic-collagen scaffolds loaded with human adipose-tissue derived stem cells for bone tissue engineering. *Molecular Biology Reports*, 41(2), 741–749. <https://doi.org/10.1007/s11033-013-2913-8>
- De Santana, R. B., de Mattos, C. M. L., Francischone, C. E., & Van Dyke, T. (2010). Superficial topography and porosity of an absorbable barrier membrane impacts soft tissue response in guided bone regeneration. *Journal of Periodontology*, 81(6), 926–933. <https://doi.org/10.1902/jop.2010.090592>
- Desmiaty, Y., Fahleni, F., Griselda, A., & Apriliana, A. Z. (2024). Enhanced ability of agarwood leaves (*Aquilaria malaccensis* Lam.) ointment as wound healing to heal second-degree burns in rats. *Sciences of Pharmacy*.
- Donos, N., Dereka, X., & Mardas, N. (2015). Experimental models for guided bone regeneration in healthy and medically compromised conditions. *Periodontology* 2000, 68(1), 99–121. <https://doi.org/10.1111/prd.12077>
- El-Shanshory, A. A., Agwa, M. M., Abd-Elhamid, A. I., Soliman, H. M. A., Mo, X., & Kenawy, E. R. (2022). Metronidazole topically immobilized electrospun nanofibrous scaffold: Novel secondary intention wound healing accelerator. *Polymers*, 14(3). <https://doi.org/10.3390/polym14030454>
- Farazin, A., & Mahjoubi, S. (2024). Dual-functional hydroxyapatite scaffolds for bone regeneration and precision drug delivery. *Journal of the Mechanical Behavior of Biomedical Materials*, 157(September), 1–7. <https://doi.org/10.1016/j.jmbbm.2024.106661>
- Grant, K. (2009). Wounds. Rat guide: A guide to health, medication use, breeding, and care of rats. Rat Guide. Retrieved October 12, 2023, from <https://ratguide.com/health/trauma/wounds.php>
- Hatakeyama, W., Taira, M., Takafuji, K., Kihara, H., & Kondo, H. (2013). Bone-regeneration trial of rat critical-size calvarial defects using nano-apatite/collagen composites. *Nano Biomedicine*, 5(2), 98–103.
- Jiang, Z., Zheng, Z., Yu, S., Gao, Y., Ma, J., Huang, L., & Yang, L. (2023). Nanofiber scaffolds as drug delivery systems promoting wound healing. In *Pharmaceutics* 15(7). <https://doi.org/10.3390/pharmaceutics15071829>
- Johnson, C. T., & García, A. J. (2015). Scaffold-based anti-infection strategies in bone repair. *Annals of Biomedical Engineering*, 43(3), 515–528. <https://doi.org/10.1007/s10439-014-1205-3>



- Kashte, S., Dhumal, R., Chaudhary, P., Sharma, R. K., Dighe, V., & Kadam, S. (2021). Bone regeneration in critical-size calvarial defect using functional biocompatible osteoinductive herbal scaffolds and human umbilical cord Wharton's Jelly-derived mesenchymal stem cells. *Materials Today Communications*, 26, 102049. <https://doi.org/10.1016/j.mtcomm.2021.102049>
- Lansdown, A. B. G., Sampson, B., & Rowe, A. (2001). Experimental observations in the rat on the influence of cadmium on skin wound repair. *International Journal of Experimental Pathology*, 82(1), 35–41. <https://doi.org/10.1046/j.1365-2613.2001.08.0.x>
- Liang, H., Yin, J., Man, K., Yang, X. B., Calciolari, E., Donos, N., Russell, S. J., Wood, D. J., & Tronci, G. (2022). A long-lasting guided bone regeneration membrane from sequentially functionalised photoactive atelocollagen. *Acta Biomaterialia*, 140, 190–205. <https://doi.org/10.1016/j.actbio.2021.12.004>
- Lim, Y. S., Ok, Y. J., Hwang, S. Y., Kwak, J. Y., & Yoon, S. (2019). Marine collagen as a promising biomaterial for biomedical applications. *Marine Drugs*, 17(8). <https://doi.org/10.3390/md17080467>
- Ma, S., Adayi, A., Liu, Z., Li, M., Wu, M., Xiao, L., Sun, Y., Cai, Q., Yang, X., Zhang, X., & Gao, P. (2016). Asymmetric collagen/chitosan membrane containing minocycline- loaded chitosan nanoparticles for guided bone regeneration. *Scientific Reports*, 6(July), 1–10. <https://doi.org/10.1038/srep31822>
- Mohan, S., Karunanithi, P., Raman Murali, M., Anwar Ayob, K., Megala, J., Genasan, K., Kamarul, T., & Balaji Raghavendran, H. R. (2022). Potential use of 3D CORAGRAF- loaded PDGF-BB in PLGA microsphere seeded mesenchymal stromal cells in enhancing the repair of calvaria critical-size bone defect in rat model. *Marine Drugs*, 20(9), 1–11. <https://doi.org/10.3390/md20090561>
- Moody, C. M., Chua, B., & Weary, D. M. (2014). The effect of carbon dioxide flow rate on the euthanasia of laboratory mice. *Laboratory Animals*, 48(4), 298–304. <https://doi.org/10.1177/0023677214546509>
- Mukherjee, P., Roy, S., Ghosh, D., & Nandi, S. K. (2022). Role of animal models in biomedical research: a review. *Laboratory Animal Research*, 38(1), 18.
- Negut, I., Dorcioman, G., & Grumezescu, V. (2020). Scaffolds for Wound Healing Applications. *Polymers*, 12(9), 2010. <https://doi.org/10.3390/polym12092010>
- Ono, M., Sonoyama, W., Nema, K., Hara, E. S., Oida, Y., Pham, H. T., Yamamoto, K., Hirota, K., Sugama, K., Sebald, W., & Kuboki, T. (2014). Regeneration of calvarial defects with escherichia coli-derived rhBMP-2 adsorbed in PLGA Membrane. *Cells Tissues Organs*, 198(5), 367–376. <https://doi.org/10.1159/000356947>
- Sato, N., Handa, K., Venkataiah, V. S., Hasegawa, T., Njuguna, M. M., Yahata, Y., & Saito, M. (2020). Comparison of the vertical bone defect healing abilities of carbonate apatite,  $\beta$ -tricalcium phosphate, hydroxyapatite and bovine-derived heterogeneous bone. *Dental Materials Journal*, 39(2), 309–318. <https://doi.org/10.4012/dmj.2019-084>
- Schmitz, J. P., & Hollinger, J. O. (1986). The critical size defect as an experimental model for craniomandibulofacial nonunions. *Clinical Orthopaedics and Related Research (1976-2007)*, 205, 299-308.
- Spicer, P. P., Kretlow, J. D., Young, S., Jansen, J. A., Kasper, F. K., & Mikos, A. G. (2012). Evaluation of bone regeneration using the rat critical size calvarial defect. *Nature protocols*, 7(10), 1918-1929.
- Suvarnapathaki, S., Wu, X., Zhang, T., Nguyen, M. A., Goulopoulos, A. A., Wu, B., & Camci-Unal, G. (2022). Oxygen generating scaffolds regenerate critical size bone defects. *Bioactive Materials*, 13, 64–81. <https://doi.org/10.1016/j.bioactmat.2021.11.002>
- Togari, K., Miyazawa, K., Yagihashi, K., Tabuchi, M., Maeda, H., Kawai, T., & Goto, S. (2012). Bone regeneration by demineralized dentin matrix in skull defects of rats. *Journal of Hard Tissue Biology*, 21(1), 25–34. <https://doi.org/10.2485/jhtb.21.25>
- Wang, K. C., Yang, L. Y., Lee, J. E., Wu, V., Chen, T. F., Hsieh, S. T., & Kuo, M. F. (2022). Combination of indirect revascularization and endothelial progenitor cell transplantation improved cerebral perfusion and ameliorated tauopathy in a rat model of bilateral ICA ligation. *Stem Cell Research and Therapy*, 13(1), 1–14. <https://doi.org/10.1186/s13287-022-03196-1>
- Zain, N., & Hamdan, M. (2021). Tilapia fish collagen: Potential as halal biomaterial in tissue engineering applications. *Nusantara Halal Journal (Halal*



*awareness, opinion, research, and initiative*), 2(1), 24-32.

Zayi, N. A. M., Halim, L., Harun, A. F., & Mohamad, M. Y. (2023). Fabrication and Characterization of Fish-Derived Collagen Scaffold Loaded with Metronidazole Nanoparticle for Periodontal Bone Regeneration. *Malaysian Journal of Microscopy*, 19(2), 141-152.

Zhou, K., Azaman, F. A., Cao, Z., Brennan Fournet, M., & Devine, D. M. (2023). Bone Tissue Engineering Scaffold Optimisation through Modification of Chitosan/Ceramic Composition. *Macromol*, 3(2), 326–342. <https://doi.org/10.3390/macromol3020021>